Catena 163 (2018) 165–171

Contents lists available at ScienceDirect

Catena

journal homepage: www.elsevier.com/locate/catena

# Responses of vegetation productivity to multi-scale drought in Loess Plateau, China

Anzhou Zhao[a,b,*], Anbing Zhang[a,b,*], Sen Cao[c], Xianfeng Liu[d], Jianhong Liu[e,f], Dayu Cheng[a,b]

[a] School of Mining and Geomatics, Hebei University of Engineering, Handan 056038, Hebei, PR China
[b] Heibei Collaborative Innovation Center of the Comprehensive Development and Utilization of Coal Resource, 199 Guangming Street, Handan 056038, PR China
[c] Department of Earth and Atmospheric Sciences, University of Alberta, Edmonton T6G 2E3, Canada
[d] School of Geography and Tourism, Shaanxi Normal University, Xi'an, Shaanxi 710062, PR China
[e] Shannxi Key Laboratory of Earth Surface System and Environmental Carrying Capacity, Northwest University, Xi'an 710127, PR China
[f] College of Urban and Environmental Science, Northwest University, Xi'an 710127, PR China

ARTICLE INFO

*Keywords:*
NDVI
Drought
SPEI
Multiple temporal resolution
Loess Plateau

ABSTRACT

Drought affects land surface dynamics. Quantifying the response of vegetation productivity to variations in drought events at different time-scales is crucial for evaluating the potential impacts of climate change on terrestrial ecosystems. Utilizing the Standardized Precipitation Evapotranspiration Index (SPEI) and Normalized Difference Vegetation Index (NDVI), this study evaluated the response of vegetation productivity to different time-scales of drought (SPEI-3, SPEI-6, SPEI-12, and SPEI-24, with 3, 6, 12 and 24 months of accumulation, respectively) in the growing season (April to October), as well as the spring, summer and autumn of the Loess Plateau (LP) by the maximum Pearson correlation ($r_{max}$). Results indicated that: (1) major areas (91.49%, 88.81%, 94.41% and 79.20%) of the LP were highly controlled by drought at the different time-scales during 1982–2013. However, high spatial and seasonal differences occurred during different time-scales, with the maximum influence in summer at 3-month time (SPEI-3); (2) $r_{max}$ showed that 98.47%, 45.91%, 89.80% and 75.33% of the LP show significant correlation ($P < 0.05$) between the SPEI and vegetation productivity in the growing season, and the spring, summer and autumn; (3) vegetation productivity of arid regions responded mostly in the 3-month time (SPEI-3), and vegetation productivity of semi-arid and semi-humid regions mostly responded at the 12-month time (SPEI-12) or 24-month time (SPEI-24) in the growing season; and lastly, (4) the $r_{max}$ was higher in the 3-month time for grassland and cultivated vegetation and in the 12-month time for the shrub land, need-leaf forest and broadleaf forest.

## 1. Introduction

Drought is a natural climate phenomenon which occurs when water availability is significantly below normal levels over a long period and the supply cannot satisfy the existing demand (Vicente-Serrano et al., 2013). Recently research has shown that with global warming, the frequency and duration of droughts have increased significantly, and the impact of drought on water resources, and especially natural ecosystems, is becoming increasingly acute (Dai, 2013; Zhang et al., 2017a, 2017b). Quantifying and predicting the response of terrestrial ecosystems to drought is a crucial challenge for climate research (Vicente-Serrano et al., 2013). Understanding the responses of vegetation productivity to drought can help to improve our knowledge of the vulnerability of ecological environment to climate change (Vicente-Serrano et al., 2013). Currently, a general theory of the effects of drought on terrestrial ecosystems is lacking due to both their inherent complexity and the limited knowledge of seasonal drought impacts on vegetation productivity over multiple temporal resolutions (Knapp and Smith, 2001; Vicente-Serrano et al., 2013).

One of the major difficulties in the understanding of drought is the selection of indicative variables. Single indicative variables can hardly assess drought conditions such as drought duration, intensity, magnitude, and space-time change (Vicente-Serrano et al., 2013). In recent years, several climatic drought indices (e.g. the Palmer Drought Severity Index (PDSI) (Palmer, 1965), the Standardized Precipitation Index (SPI) (McKee et al., 1993) and the Standardized Precipitation Evapotranspiration Index (SPEI) (Vicente-Serrano et al., 2010)) have been widely used to assess drought conditions. The PDSI is based on a soil water balance equation, but this index has numerous deficiencies, including the main criticism that the PDSI has a fixed temporal scale

* Corresponding authors at: School of Mining and Geomatics, Hebei University of Engineering, Handan 056038, Hebei, PR China.
*E-mail addresses:* zhaoanzhou@126.com (A. Zhao), zhanganbing@hebeu.edu.cn (A. Zhang).

https://doi.org/10.1016/j.catena.2017.12.016
Received 27 July 2017; Received in revised form 26 October 2017; Accepted 15 December 2017
Available online 21 December 2017

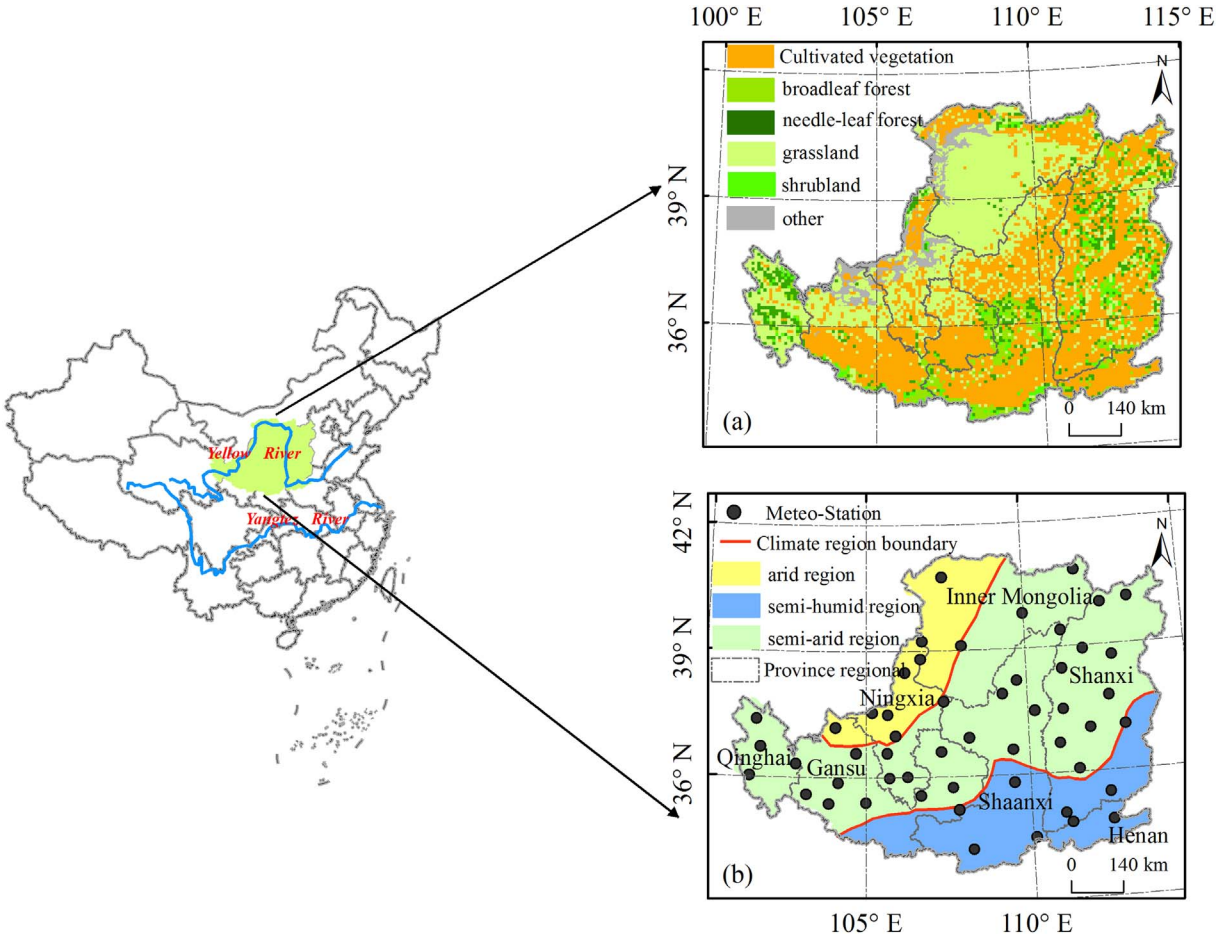


**Fig. 1.** Geographical maps of the Loess Plateau: (a) the distribution of vegetation types, (b) 52 weather stations meteorological stations and 3 climate regions.

(Vicente-Serrano et al., 2013). However, drought as a multi-scalar phenomenon has been widely accepted and used as a framework to monitor drought impacts on terrestrial ecosystems (McKee et al., 1993; Vicente-Serrano et al., 2013; De Keersmaecker et al., 2017). The SPI has been accepted by the World Meteorological Organization (WMO) as the reference drought index, due to the fact that it can be calculated at multiple temporal resolutions (Guttman, 1998). Many studies analyzed the response of vegetation activity to drought by using the SPI (Wang et al., 2015; Vicente-Serrano et al., 2006). However, the calculation of SPI only incorporates precipitation data, and other crucial factors (e.g. evapotranspiration and temperature) that can affect the frequency of drought are not included (Vicente-Serrano et al., 2010). Some studies have indicated that warming processes significantly increased evapotranspiration and increased drought stress on a regional scale (Rebetez et al., 2006; Adams et al., 2009). Because of this finding, it is important to evaluate the relationship between land surface dynamics and drought under global warming conditions (Breshears et al., 2005). SPEI was established by Vicente-Serrano et al. (2010). It is a multi-scalar drought index used to determine both water deficit and surplus at different timescales (Li et al., 2015). The SPEI is calculated from mean monthly temperature and precipitation data which has been collected from meteorological stations. This drought indicator considers the multi-scalar character of the SPI, varies in evaporation demand of the PDSI, and is better to characterize recent drought events that have occurred under climatic warming, especially in semi-arid and arid regions (Vicente-Serrano et al., 2013).

The Normalized Difference Vegetation Index (NDVI) is a good indicator for monitoring vegetation productivity and has been widely used to assess vegetation degradation, ecosystem features, and the physiologic drought conditions of vegetation and patterns of vegetation productivity (Zhang et al., 2013; Wang et al., 2003). The third-generation Global Inventory Modeling and Mapping Studies (GIMMS3g) with a 1/12° spatial resolution is considered an ideal dataset to analyze the relationships between climate variability and land surface dynamics for long time series and large-scale areas. Using the GIMMS3g dataset, Gouveia et al. (2017) analyzed drought impacts on NDVI in the entire Mediterranean basin. They found large areas of Mediterranean basin highly controlled by drought. Zhang et al. (2017a) evaluated the response of vegetation to multiple temporal resolution droughts across China, and showed that vegetation productivity and SPEI were significantly positively correlated in most regions of China.

The Loess Plateau is an important agricultural region and covers a large area in the northwest of China (Liu et al., 2016). Drought hazards frequently occur and affect the healthy and sustainable development of agricultural, socio-economic and ecological environment (Shi and Shao, 2000; Liu et al., 2016). Zhang et al. (2016) analyzed the responses of vegetation cover to drought in the Loess Plateau (LP). They found that vegetative growth was responsive to droughts (SPEI-12, 12 months of accumulation.). However, only SPEI-12 was taken into account in the study of vegetation response to drought. Responses of vegetation activity to seasonal droughts were not included in the study. With observed increases in global intensity and frequency of drought under climate change conditions, knowledge of the impact in terrestrial ecosystems is crucial, especially as it pertains to vegetation responses to drought events, so that future projections of climate change can be planned for. However, few studies have evaluated the impact of seasonal droughts on land surface dynamics, and there are still many uncertainties regarding the sensitivity of vegetation to seasonal droughts over different time-scales at regional scale processes in the LP.

In this context, the aim of the present study is to analyze the effects

of the seasonality of drought events on the vegetation of different types in the LP. SPEI of different time-scales (3, 6, 12 and 24 months) from 1982 to 2013 is calculated as climatic drought index using meteorological data at 52 weather stations. Corresponding NDVI data are derived as proxies of vegetation productivity from GIMMS NDVI3g dataset. Finally, SPEI of different time scales is related to NDVI values using Pearson correlation analysis.

## 2. Materials and methods

### 2.1. Study area

The LP (104°54′E to 114°33′E, 33°43′N to 41°16′N) is located in the middle reaches of the Yellow River in China and covers approximately 620,000 km$^2$. It includes most parts of Shaanxi and Shanxi, as well as Ningxia, and parts of Qinghai, Gansu, Henan and Inner Mongolia. Its undulating terrain varies in elevation from 200 to 3000 m. This region is dominated by a temperate continental monsoon climate, and semi-humid, semi-arid and arid areas that were subcategorized from southeast to northwest (Xie et al., 2016) (Fig. 1b). The mean annual precipitation ranges from 150 mm/yr in the northwest to 800 mm/yr in the southeast. The mean annual temperature ranges from 4.3 °C in the northwest to 14.3 °C in the southeast (Zhao et al., 2017a). We defined spring, summer, autumn and the growing season as March to May, June to August, September to November, and April to October, respectively (Zhao et al., 2017b). The dominant vegetation types include broad-leaved forest, needle-leaf forest, grassland, shrub land and cultivated vegetation. Due to the uneven distribution of precipitation, intensive human activity and strong evaporation, the LP has suffered from severe drought, serious soil erosion, and desertification (Fig. 1a) (Zhao et al., 2017b).

### 2.2. Data

The GIMMS NDVI3g dataset was generated from the NOAA-AVHRR (Advanced Very High Resolution Radiometer) sensor for the period from July 1981 to December 2013. This dataset has been corrected for orbital drift effects and volcanic eruptions, as well as other errors unrelated to vegetation change (Pinzon and Tucker, 2014), and has been verified and extensively applied (Luo et al., 2014; Wang et al., 2015). The spatial resolution of the data is 1/12° and the temporal resolution is 15 days (Guay et al., 2014). Maximum value composite (MVC) technique was employed to calculate the monthly GIMMS NDVI3g dataset. It should be noted that the NDVI value for each meteorological station was calculated as the average of its 3 × 3 neighbors to remove the possible misalignments between the two datasets.

Meteorological datasets employed in this study include monthly precipitation and mean monthly temperature from 52 meteorological stations from 1982 to 2013 spatially distributed across the LP. These data were collected from the China Meteorological Sharing Service System (http://cdc.cma.gov.cn/). The reliability and homogeneity of the monthly meteorological data were controlled and checked by the Chinese Meteorological Administration before its release (Yu et al., 2014).

We used a vegetation map (vector data) with a scale of 1:1,000,000 which was created in 2001 as a part of the Atlas of China's Vegetation. The vector data were converted into raster format at a 1/12° spatial resolution. In the map, vegetation was classified into needle-leaf forest, broad-leaved forest, shrub land, cultivated vegetation, steppe, meadow, marshy grassland, and desert. In this study, needle-leaf forest, broad-leaved forest, shrub land, cultivated vegetation and grassland were selected to analyze the relationship between vegetation activity and drought.

### 2.3. SPEI drought indicator

To calculate SPEI, the monthly difference between precipitation (P) and potential evapotranspiration (PET) is used in, the Thornthwaite method to calculate the PET (Thornthwaite, 1948). With calculate value for P and PET, the difference between P and PET for the month $i$ is calculated as follows:

$$D_i = P_i - PET_i \quad (1)$$

The calculated $D$ values are aggregated at various time scales:

$$D_n^k = \sum_{i=0}^{k-1} (P_{n-i} - PET_{n-i}),\ n \geq k \quad (2)$$

where $P$ is precipitation, $PET$ is the potential evapotranspiration calculated by Thorthwaite method, $k$ (months) and $n$ is the timescale of the aggregation and the calculation number, respectively. $D_n^k$ is based on both the $n^{th}$ climatic water balance and the water balance for the preceding $k$-1 months. For example, the 3-month SPEI is constructed by the sum of $D$ values from two previous months to the current month. The criteria for drought classification based on SPEI values are referenced as defined in McKee et al. (1993) and Potopová et al. (2015).

To improve our understanding of the relationship between land surface dynamics and drought at multiple-time scales from 3 to 24 months, SPEI-3, SPEI-6, SPEI-12 and SPEI-24 from 1982 to 2013 was calculated as a proxy of drought representing short (3 months), medium (6 months), medium–long (12 months), and long time-scales (24 months), respectively (Liu et al., 2016; Hua et al., 2017).

### 2.4. Statistical analysis

Pearson correlation (PC) analysis was calculated between monthly (March to November) NDVI series at different time-scales (3, 6, 12, and 24 months) as follows (Zhang et al., 2017a):

$$r_{i,j} = corr\,(NDVI_i, SPEI_{i,j}) \quad 3 \leq i \leq 11,\ j = 3,\ 6,\ 12,\ 24 \quad (3)$$

$$r_{\max} = \max_{3\leq i\leq 11, j=3,6,12,24}(r_{i,j}) \quad (4)$$

where *corr* represents the PC; $i$ is the $i$th month and ranges from 3th to 11st; $j$ represents the drought time-scale and its value is 3, 6, 12 or 24 month; *NDVIi* and *SPEIi,j* are the $i$th month NDVI series and the $i$th month drought index with a time-scale of $j$ months; and *ri,j* and *rmax* are the PC between *NDVIi* and *SPEIi,j* and the maximum correlation coefficient. The total length of observations in our study is 32 years, giving a PC value of 0.35 a significance level of 0.05.

As a result, we had 36 (9 months × 4 time-scales) *ri,j* values for each meteorological station. To assess the impact of the drought on vegetation productivity in spring, summer, autumn, and growing season, respectively, the maximum value ($r_{max}$) were derived from monthly correlations for each season (Zhang et al., 2017a; Vicente-Serrano et al., 2013). Further interpolation of the surface data was performed using the Inverse Distance Weighted (IDW) method to achieve a final resolution of 1/12° (Bartier and Keller, 1996).

## 3. Results

### 3.1. Spatial distribution of the $r_{max}$ for growing season, spring, summer and autumn, using the multiple temporal resolution

Fig. 2 indicates the spatial distribution of $r_{max}$ between vegetation productivity and SPEI for the spring, summer, autumn and the growing season, at the temporal scales of 3, 6, 12 and 24 months. Excluding bare lands, water and marsh, during the growing season, vegetation productivity was significantly and positively correlated ($P < 0.05$) with SPEI in about 91.49%, 88.81%, 94.41% and 79.20% of the LP at the different SPEI time-scales (Table 1). The higher correlations are found at for the temporal resolution of 3, 6, 12, 24 months in almost all the

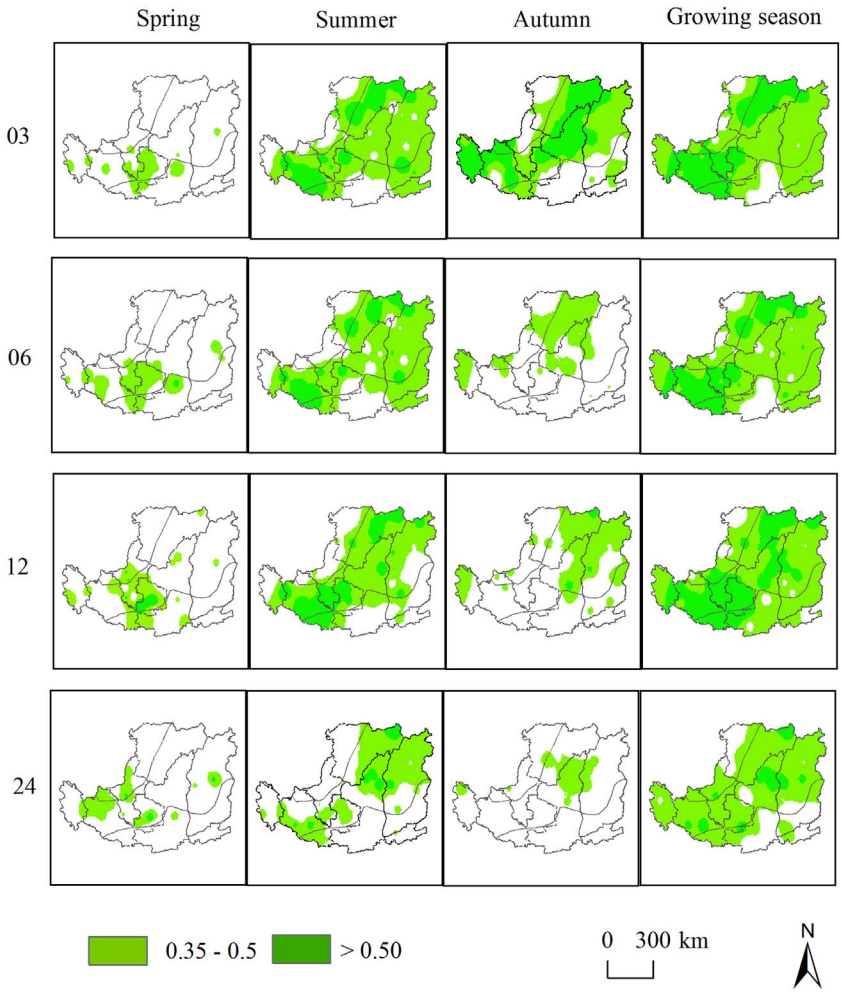


**Fig. 2.** Spatial distribution of correlations between SPEI and vegetation productivity for spring, summer, autumn, and growing season, using the temporal resolution of 3, 6, 12 and 24 months. Non-significant areas were given white color.

**Table 1**
Area percentage of the present significant ($P < 0.05$) correlations for different time scales in the LP. Bare land, water, and marsh areas are not included.

| | 03 | 06 | 12 | 24 | $r_{max}$ |
|---|---|---|---|---|---|
| Spring | 10.24% | 17.56% | 17.25% | 10.16% | 45.91% |
| Summer | 82.76% | 76.32% | 69.38% | 43.89% | 89.80% |
| Autumn | 60.06% | 28.15% | 35.54% | 12.05% | 75.33% |
| Growing season | 91.49% | 88.81% | 94.41% | 79.20% | 98.47% |

LP. These results indicated a close relationship between vegetation and drought events. During the three seasons, there are obviously differences between the vegetation productivity and SPEI correlations considering the different SPEI time-scales. In spring, vegetation productivity was significantly and positively correlated ($P < 0.05$) with SPEI in about 10.24%, 17.56%, 17.25% and 10.16% of the LP for the different SPEI time-scales (Table 1). The significant values were concentrated on semi-arid regions including southern Ningxia province and eastern Gansu province, respectively, where vegetation types are mainly grassland and cultivated vegetation (Fig. 2). In the summer, vegetation productivity was significantly and positively correlated ($P < 0.05$) with SPEI in about 82.76%, 76.32%, 69.38% and 43.89% of the LP for the different SPEI time-scales (Table 1). They presented higher significant and positive correlations ($P < 0.05$) for the shortest (3 months) and medium time scales (6 months). The higher correlations found at 3 and 6 months in almost all the LP are in contrast with correlations at 12 and 24 months, where are concentrated in semi-arid regions of the northern and southwest LP, respectively. In those areas, the cultivated vegetation dominated the landscape. In the autumn, the correlation between the SPEI and the vegetation productivity are particularly strong at the 3-month time due to the low water balance (Fig. 2). 60.06%, 28.15%, 35.54% and 12.05% of the vegetated land areas show a significant correlation between the vegetation productivity and the different SPEI time-scales in autumn (Table 1).

To analyze the strongest relationship between vegetation productivity and SPEI in the spring, summer, autumn, and growing season, we selected the $r_{max}$ of significant ($P < 0.05$) correlations between vegetation productivity and *S*PEI for the different *S*PEI time-scales (3, 6, 12 and 24 months) (Fig. 3). In the growing season, vegetation productivity correlates with drought throughout almost all the LP (Fig. 3). Vegetation productivity of the land covers except bare land, water, and marsh areas was significantly and positively correlated ($P < 0.05$) with SPEI in about 98.47% of the LP during 1982–2013 (Table 1). However, the influence of drought on vegetation productivity changed markedly with the season and among regions. In the summer and autumn, the correlation between the vegetation productivity and the SPEI data are particularly strong throughout large regions (e.g., in northern Shaanxi, Shanxi and eastern Gansu provinces) (Fig. 3). In the spring, the correlation between the vegetation productivity and the SPEI data are particularly strong throughout the east of Gansu province (Fig. 3). Overall, 45.91%, 89.80%, 75.33% and 98.47% of the LP (except for bare land, water, and marsh) showed a significant correlation between the SPEI and NDVI in the spring, summer, autumn and the growing season (Table 1).

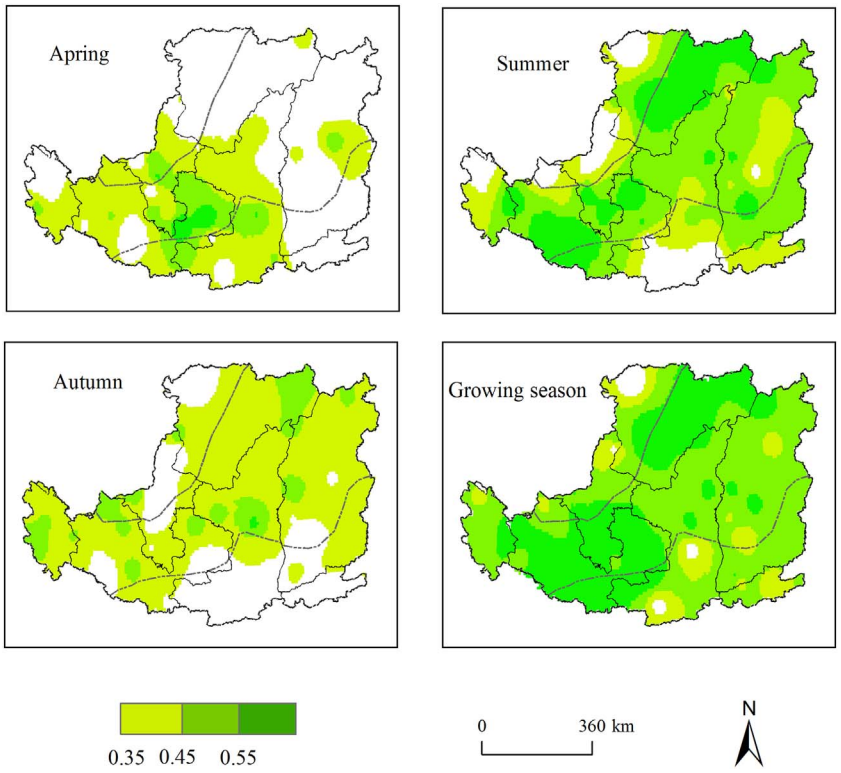


**Fig. 3.** Spatial distribution of the maximum correlation coefficients between the monthly NDVI series and the monthly SPEI series at the time-scale of 3, 6, 12, and 24 months, during spring, summer, autumn, and growing season. Non-significant areas were given white color.

### 3.2. Response of vegetation productivity to drought seasonality at different time-scales

Fig. 4 shows the spatial distribution of $r_{max}$ at each station for the different SPEI time-scales (3, 6, 12 and 24 months). In the growing season, we found 16 stations (around 32% of all stations), vegetation productivity are significantly affected by drought at both short and medium time-scales (i.e., SPEI-3 and SPEI-6) and spread across the north (arid region) of the LP. However, at 32 stations (about 61.5% of the all stations), vegetation productivity are significantly affected by drought at both 12-month time and 24-month time (i.e., SPEI-12 and SPEI-24) and spread over the middle part (semi-arid region) and south

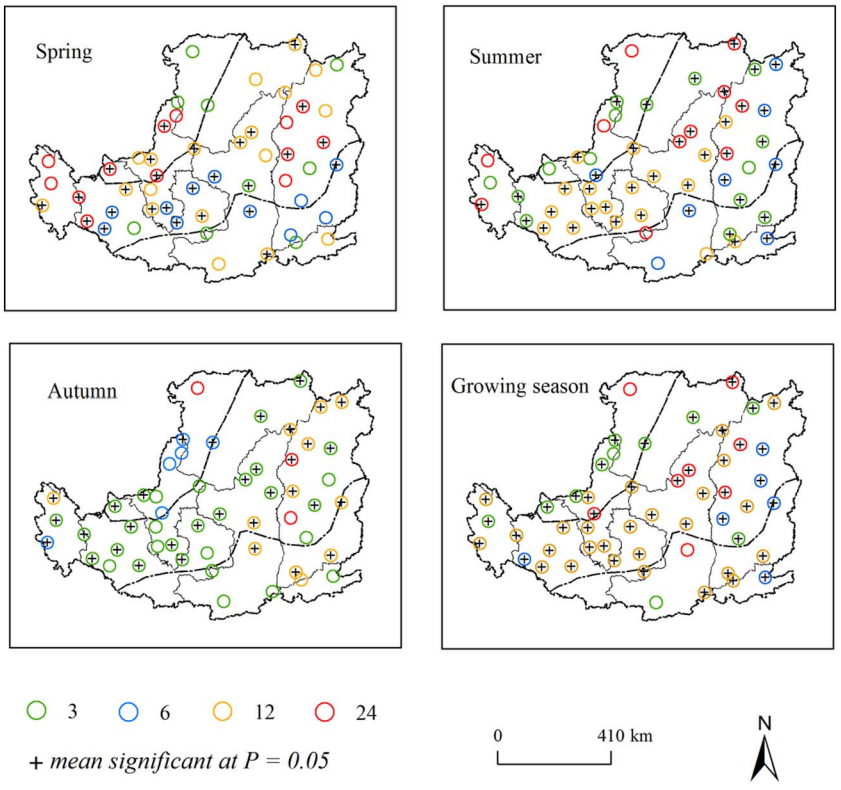


**Fig. 4.** Time scale of the SPEI showing the maximum correlation with the vegetation productivity in the meteorological stations of LP.

(semi-humid region) of the LP (Fig. 4). In the spring, 17.3% of the stations' NDVI are significantly affected by drought at 3-month time and 6-month time (central Shaanxi and east of Gansu provinces) and 36% of the stations vegetation productivity are significantly affected by the 12-month time and 24-month time (in northern Shaanxi and Shanxi, western Ningxia provinces). In the summer, we found that 9 and 7 stations, which accounted for 17.3% and 13.5% of the total, were significantly affected by the 3-month time and 6-month time, respectively. Those stations were mainly distributed in the Shanxi province and northern LP. At the 12-month time and 24-month time, 17 and 8 stations, which accounted for 32.7% and 15.4% of the total number of stations, were significantly affected by droughts, and were mainly distributed in the middle of the LP. In the autumn, we found that 19 and 3 stations, which accounted for 36.5% and 5.8% of the total, were significantly affected by the 3-month time and 6-month time, respectively. Those stations were mainly distributed in the north of Shanxi, east of Gansu and south of Ningxia. At the 12-month time-scale, 11 stations distributed in Shanxi (21.2% of the total) were significantly affected by droughts; and at the 24-month time-scale, 1 station distributed in central Shaanxi (1.9% of the total) were significantly affected by droughts.

### 3.3. Correlation between droughts and SPEI for different land cover types

The $r_{max}$ between the vegetation productivity of different land cover types and drought events were evaluated at different time-scales. Table 2 indicates that the $r_{max}$ was higher for grassland at all the time-scales (SPEI-3, SPEI-6, SPEI-12, and SPEI-24), with mean values of 0.499, 0.472, 0.486 and 0.472, respectively. The $r_{max}$ was lower for needle-leaf forest, with mean values of 0.441, 0.435, 0.455,and 0.432 at SPEI-3, SPEI-6, SPEI-12 and SPEI-24 (Table 2). The $r_{max}$ between the vegetation productivity at all time-scales could reflect the responses of vegetation to drought in general, as all the vegetation types had high significance. For grassland, the mean $r_{max}$ was 0.499, 0.472, 0.486 and 0.472 at SPEI-3, SPEI-6, SPEI-12 and SPEI-24 time-scales, respectively. The $r_{max}$ was 0.475, 0.445, 0.462 and 0.451 for cultivated vegetation at all time-scales, which indicated that grassland and cultivated vegetation were more correlated to 3-month time-scale of drought (SPEI-3). The mean $r_{max}$ was 0.455, 0.452, 0.464 and 0.463 for shrub land, 0.441, 0.435, 0.455 and 0.432 for needle-leaf forest, and 0.456, 0.438, 0.469 and 0.432 for broadleaf forest at all time-scales, respectively. Across those vegetation types, the maximum correlation was at the 12-month time (SPEI-12).

**Table 2**
The statistic of $r_{max}$ between SPEI and vegetation activity for different vegetation types at the time-scale of 3, 6, 12, and 24 months.

| | Type of vegetation | Max | Min | Mean | Standard deviation |
|---|---|---|---|---|---|
| SPEI-3 | Grassland | 0.786 | 0.134 | 0.499 | 0.077 |
| | Shrub land | 0.687 | 0.123 | 0.455 | 0.057 |
| | Cultivated vegetation | 0.704 | 0.141 | 0.475 | 0.086 |
| | Need-leaf forest | 0.662 | 0.122 | 0.441 | 0.088 |
| | Broadleaf forest | 0.654 | 0.163 | 0.456 | 0.077 |
| SPEI-6 | Grassland | 0.733 | 0.178 | 0.472 | 0.074 |
| | Shrub land | 0.640 | 0.202 | 0.452 | 0.056 |
| | Cultivated vegetation | 0.698 | 0.165 | 0.445 | 0.090 |
| | Need-leaf forest | 0.654 | 0.201 | 0.435 | 0.080 |
| | Broadleaf forest | 0.646 | 0.229 | 0.438 | 0.085 |
| SPEI-12 | Grassland | 0.685 | 0.190 | 0.486 | 0.066 |
| | Shrub land | 0.661 | 0.322 | 0.464 | 0.055 |
| | Cultivated vegetation | 0.691 | 0.179 | 0.462 | 0.088 |
| | Need-leaf forest | 0.658 | 0.330 | 0.455 | 0.058 |
| | Broadleaf forest | 0.639 | 0.255 | 0.469 | 0.074 |
| SPEI-24 | Grassland | 0.624 | 0.166 | 0.472 | 0.053 |
| | Shrub land | 0.621 | 0.241 | 0.463 | 0.066 |
| | Cultivated vegetation | 0.624 | 0.132 | 0.451 | 0.082 |
| | Need-leaf forest | 0.585 | 0.269 | 0.432 | 0.072 |
| | Broadleaf forest | 0.619 | 0.251 | 0.432 | 0.076 |

## 4. Discussion

The LP has been considered the most important agricultural region in China-for thousands of years, and has been historically sensitive to changes in climate, experiencing a long-term warming-drying climatic trend with declining precipitation and increasing temperature over the past few decades (Wang et al., 2011; Yao et al., 2013; Sun et al., 2015). The high risk of drought impacts on agricultural and natural ecosystems and the consequent risks of land desertification and soil degradation is notorious across the region. In the past few decades, a great number of studies have reported that the severity and frequency of drought have exhibited an overall increasing trend across the LP (Jiang et al., 2015; Yao et al., 2013; Liu et al., 2016; Zhang et al., 2016; Zhang et al., 2017b). When used across multiple time scales, the SPEI is an effective drought index that could contain information on evapotranspiration in drought monitoring, thereby making it possible to reflect the changes in water demands in arid and semiarid regions, especially under the background of global warming (Potop et al., 2012; Liu et al., 2016). In this study, we used a time-series of 32-yr NDVI data and a multiple-scale drought index-SPEI to assess responses of vegetation productivity to multi-scale drought in the LP. In the growing season, summer and autumn, correlation coefficients between monthly values of SPEI and monthly vegetation productivity were highly significant ($r > 0.35$) in the middle of LP (Fig. 3). In the southern LP, vegetation activity was less sensitive ($r < 0.35$) to drought due to relatively high precipitation. Temperature and other climate factors might be the controls in this area. In a region with lower annual precipitation, such as the northwest LP, there were also lower correlations ($r < 0.35$) between monthly values of SPEI and monthly NDVI, potentially because of the major controls on vegetation activity through the water supply provided by inland rivers, or ground water availability. These results agree with those obtained by Hua et al. (2017) and Vicente-Serrano et al. (2013).

We also studied the responses of the different vegetation types to drought based on the NDVI and SPEI time scales across the LP. The responses of vegetation to drought are different for different vegetation types, and these responses were analyzed based on the $r_{max}$ between monthly values of SPEI and monthly NDVI for multiple SPEI time-scales (3, 6, 12 and 24 months). For the broadleaf forest, needle-leaved forest and shrub-land, the $r_{max}$ was higher for the 12-month time (SPEI-12) (Table 2). This is probably because these specific vegetation types are mainly local in the southern of LP with relatively high precipitation. Those vegetation types could be insensitive to SPEI-3, but their physiological structure could be affected at 12-month time-scale (SPEI-12). Drought impacts on these vegetation types at 3-month time-scale could have been mitigated due to their deeper root systems and water conservation methods. However, for cultivated vegetation and grassland areas, the $r_{max}$ was higher at 3-month time-scale (SPEI-3) (Table 2). This may occur because these vegetation types are mainly localized in the north and middle of the LP, or areas with relatively less precipitation. Those vegetation types could be sensitive to short droughts and have functional strategies and physiological anatomy enabling them to adapt rapidly to varying water availability. Our results are similar to those of previous studies which analyzed the drought situation in China (Li et al., 2015; Hua et al., 2017; Zhang et al., 2017a).

In this study, the response of different vegetation types to drought at multiple temporal resolution in the LP was analyzed. The aridity and associated climatic and geographic characteristics could also help explain the spatial differences of the drought. However, other factors (e.g., ecological restoration, agricultural irrigation, soil proprieties and topography) also could affect land surface dynamics. Due to the large spatial heterogeneity of the LP, other studies are needed to assess the impact of local conditions (e.g., topography and agricultural irrigation) on the vegetation's responses to the drought at multiple temporal-scales (Gouveia et al., 2017). Other studies have indicated that water balance

also affected the geographical distribution of vegetation types (Vicente-Serrano et al., 2013; Wu et al., 2015). This work would be done in the future. Nevertheless, our findings are valuable for ecological assessments, drought management and understanding the impacts of drought on different vegetation types, and represent one of the largest generalized drought studies on multiple vegetation types and multiple timescales.

## 5. Conclusions

In this study, the relationship between drought occurrence and vegetation activity in the LP was assessed by using the monthly values of SPEI and monthly NDVI at different time-scales ranging from 3 to 24 months, and the impacts of these time-scales on different vegetation types was analyzed. Our results indicated that vegetation productivity was significantly and positively correlated ($P < 0.05$) with SPEI in most of the LP for the different time-scales (3, 6, 12, and 24 months, respectively) in the past three decades. Among the three seasons (spring, summer, autumn, and growing season) examined, for the summer and autumn, correlations between the vegetation productivity and the SPEI data were particularly strong in northern Shaanxi, Shanxi, and eastern Gansu provinces. For the spring, correlations between the vegetation productivity and the SPEI data were particularly strong in the northwest LP. Among the five vegetation types (grassland, shrub land, cultivated vegetation, need-leaf forest, and broadleaf forest), $r_{max}$ was higher in the 3-month time (SPEI-3) for grassland and cultivated vegetation, but for the shrub land, needle-leaf forest and broadleaf forest, the $r_{max}$ was higher in the 12-month time (SPEI-12). In the growing season, vegetation in an arid region seems to respond to drought mostly at 3-month time, and the vegetation in a semi-arid and semi-humid region seems to respond to drought mostly at the 12-month time or 24-month time. Our findings are important for future climate change, drought monitoring, land surface dynamics, and hydrological studies in the LP.

## Acknowledgments

The work was partially supported by the National Key Research and Development Program of China (Grant # 2017YFB0503602), Natural Science Foundation of Hebei Province (Grant # D2017402159) and National High Technology Research and Development Program 863 of China (Grant # 2015AA123901).

## References

Adams, H.D., Guardiola-Claramonte, M., Barron-Gafford, G.A., Villegas, J.C., Breshears, D.D., Zou, C.B., Troch, P.A., Huxman, T.E., 2009. Temperature sensitivity of drought-induced tree mortality portends increased regional die-off under global-change-type drought. P. Natl. Acad. Sci. USA. 106 (17), 7063–7066.

Bartier, P.M., Keller, C.P., 1996. Multivariate interpolation to incorporate thematic surface data using inverse distance weighting (IDW). Comput. Geosci-UK. 22 (7), 795–799.

Breshears, D.D., Cobb, N.S., Rich, P.M., Price, K.P., Allen, C.D., Balice, R.G., Romme, W.H., Kastens, J.H., Lisa, Floyd M., Belnap, J., Anderson, J.J., Myers, O.B., Anderson, J.J., 2005. Regional vegetation die-off in response to global-change-type drought. P. Natl. Acad. Sci. USA. 102 (42), 15144–15148.

Dai, A., 2013. Increasing drought under global warming in observations and models. Na. Clim. Change. 3 (1), 52–58.

De Keersmaecker, W., Lhermitte, S., Hill, M.J., Tits, L., Coppin, P., Somers, B., 2017. Assessment of regional vegetation response to climate anomalies: a case study for Australia using GIMMS NDVI time series between 1982 and 2006. Remote Sens. 9 (1), 34.

Gouveia, C.M., Trigo, R.M., Beguería, S., Vicente-Serrano, S.M., 2017. Drought impacts on vegetation activity in the Mediterranean region: an assessment using remote sensing data and multi-scale drought indicators. Glob. Planet. Chang. 151, 15–27.

Guay, K.C., Beck, P.S., Berner, L.T., Goetz, S.J., Baccini, A., Buermann, W., 2014. Vegetation productivity patterns at high northern latitudes: a multi-sensor satellite data assessment. Glob. Chang. Biol. 20 (10), 3147–3158.

Guttman, N.B., 1998. Comparing the Palmer drought index and the standardized precipitation index. J. Am. Water Resour. Assoc. 34 (1), 113–121.

Hua, T., Wang, X.M., Zhang, C.X., Liang, L.L., Li, H., 2017. Responses of vegetation activity to drought in northern China. Land Degrad. Dev. 28 (7), 1913–1921.

Jiang, R.G., Xie, J.C., He, H.L., Luo, J.G., Zhu, J.W., 2015. Use of four drought indices for evaluating drought characteristics under climate change in Shaanxi, China: 1951–2012. Nat. Hazards 75 (3), 2885–2903.

Knapp, A.K., Smith, M.D., 2001. Variation among biomes in temporal dynamics of aboveground primary production. Science 291 (5503), 481–484.

Li, Z., Zhou, T., Zhao, X., Huang, K.C., Gao, S., Wu, T., Luo, H., 2015. Assessments of drought impacts on vegetation in china with the optimal time scales of the climatic drought index. Int. J. Environ. Res. Public Health 12 (7), 7615–7634.

Liu, Z.P., Wang, Y.Q., Shao, M.G., Jia, X.X., Li, X.L., 2016. Spatiotemporal analysis of multiscalar drought characteristics across the Loess Plateau of China. J. Hydrol. 534, 281–299.

Luo, X.Z., Chen, X.Q., Wang, L.X., Xu, L., Tian, Y.H., 2014. Modeling and predicting spring land surface phenology of the deciduous broadleaf forest in northern China. Agric. For. Meteorol. 198, 33–41.

McKee, T.B., Doesken, N.J., Kleist, J., 1993. The relationship of drought frequency and duration to time scales. Proceedings of the 8th Conference on Applied Climatology. Boston, MA. Am. Meteorol. Soc. 17 (22), 179–183.

Palmer, W.C., 1965. Meteorological Drought. US Department of Commerce, Weather Bureau, Washington, DC.

Pinzon, J.E., Tucker, C.J., 2014. A non-stationary 1981–2012 AVHRR NDVI3g time series. Remote Sens. 6 (8), 6929–6960.

Potop, V., Možný, M., Soukup, J., 2012. Drought evolution at various time scales in the lowland regions and their impact on vegetable crops in the Czech Republic. Agric. For. Meteorol. 156, 121–133.

Potopová, V., Štěpánek, P., Možný, M., Türkott, L., Soukup, J., 2015. Performance of the standardised precipitation evapotranspiration index at various lags for agricultural drought risk assessment in the Czech Republic. Agric. For. Meteorol. 202, 26–38.

Rebetez, M., Mayer, H., Dupont, O., Schindler, D., Gartner, K., Kropp, J.P., Menzel, A., 2006. Heat and drought 2003 in Europe: a climate synthesis. Ann. For. Sci. 63 (6), 569–577.

Shi, H., Shao, M.G., 2000. Soil and water loss from the Loess Plateau in China. J. Arid Environ. 45 (1), 9–20.

Sun, W.Y., Song, X.Y., Mu, X.M., Gao, P., Wang, F., Zhao, G.J., 2015. Spatiotemporal vegetation cover variations associated with climate change and ecological restoration in the Loess Plateau. Agric. For. Meteorol. 209, 87–99.

Thornthwaite, C.W., 1948. An approach toward a rational classification of climate. Geogr. Rev. 38 (1), 55–94.

Vicente-Serrano, S.M., Cuadrat-Prats, J.M., Romo, A., 2006. Early prediction of crop production using drought indices at different time-scales and remote sensing data: application in the Ebro Valley (north-east Spain). Int. J. Remote Sens. 27 (3), 511–518.

Vicente-Serrano, S.M., Beguería, S., López-Moreno, J.I., 2010. A multiscalar drought index sensitive to global warming: the standardized precipitation evapotranspiration index. J. Clim. 23 (7), 1696–1718.

Vicente-Serrano, S.M., Gouveia, C., Camarero, J.J., Beguería, S., Trigo, R., López-Moreno, J.I., Azorín-Molina, C., Pasho, E., Lorenzo-Lacruz, J., Revuelto, J., Morán-Tejeda, E., Sanchez-Lorenzo, A., 2013. Response of vegetation to drought time-scales across global land biomes. P. Natl. Acad. Sci. USA. 110 (1), 52–57.

Wang, J., Rich, P.M., Price, K.P., 2003. Temporal responses of NDVI to precipitation and temperature in the central Great Plains, USA. Int. J. Remote Sens. 24 (11), 2345–2364.

Wang, Y.Q., Shao, M.A., Zhu, Y.J., Liu, Z.P., 2011. Impacts of land use and plant characteristics on dried soil layers in different climatic regions on the Loess Plateau of China. Agric. For. Meteorol. 151 (4), 437–448.

Wang, H.L., Chen, A.F., Wang, Q.F., He, B., 2015. Drought dynamics and impacts on vegetation in China from 1982 to 2011. Ecol. Eng. 75, 303–307.

Wu, D.H., Zhao, X., Liang, S.L., Zhou, T., Huang, K.C., Tang, B.J., Zhao, W.Q., 2015. Time-lag effects of global vegetation responses to climate change. Glob. Chang. Biol. 21 (9), 3520–3531.

Xie, B.N., Jia, X.X., Qin, Z.F., Shen, J., Chang, Q.R., 2016. Vegetation dynamics and climate change on the Loess Plateau, China: 1982–2011. Reg. Environ. Chang. 16 (6), 1583–1594.

Yao, Y.B., Wang, R.Y., Yang, J.H., Yue, P., Lu, D.R., Xiao, G.J., Wang, Y., Liu, L.C., 2013. Changes in terrestrial surface dry and wet conditions on the Loess Plateau (China) during the last half century. J. Arid. Land 5 (1), 15–24.

Yu, M.X., Li, Q.F., Hayes, M.J., Svoboda, M.D., Heim, R.R., 2014. Are droughts becoming more frequent or severe in China based on the standardized precipitation evapotranspiration index: 1951–2010? Int. J. Climatol. 34 (3), 545–558.

Zhang, Y.L., Gao, J.G., Liu, L.S., Wang, Z.F., Ding, M.J., Yang, X.C., 2013. NDVI-based vegetation changes and their responses to climate change from 1982 to 2011: a case study in the Koshi River Basin in the middle Himalayas. Glob. Planet. Chang. 108, 139–148.

Zhang, B.Q., He, C.S., Burnham, M., Zhang, L.H., 2016. Evaluating the coupling effects of climate aridity and vegetation restoration on soil erosion over the Loess Plateau in China. Sci. Total Environ. 539, 436–449.

Zhang, Q., Kong, D.D., Singh, V.P., Shi, P.J., 2017a. Response of vegetation to different time-scales drought across China: spatiotemporal patterns, causes and implications. Glob. Planet. Chang. 152, 1–11.

Zhang, B.Q., Wang, Z.K., Chen, G., 2017b. A sensitivity study of applying a two-source potential evapotranspiration model in the standardized precipitation evapotranspiration index for drought monitoring. Land Degrad. Dev. 28 (2), 783–793.

Zhao, A.Z., Zhang, A.B., Liu, X.F., Cao, S., 2017a. Spatiotemporal changes of normalized difference vegetation index (NDVI) and response to climate extremes and ecological restoration in the Loess Plateau, China. Theor. Appl. Climatol. 1–13. http://dx.doi.org/10.1007/s00704-017-2107-8.

Zhao, A.Z., Zhang, A.B., Lu, C.Y., Wang, D.L., Wang, H.F., Liu, H.X., 2017b. Spatiotemporal variation of vegetation coverage before and after implementation of Grain for Green Program in Loess Plateau, China. Ecol. Eng. 104, 13–22.